

Time constant determination for electrical equivalent of biological cells

Ashutosh Kumar Dubey, Shourya Dutta-Gupta, Ravi Kumar, Abhishek Tewari, and Bikramjit Basu^{a)}

Department Materials and Metallurgical Engineering, Indian Institute of Technology, IIT Kanpur, 208016 India

(Received 29 September 2008; accepted 16 January 2009; published online 29 April 2009)

The electric field interactions with biological cells are of significant interest in various biophysical and biomedical applications. In order to study such important aspect, it is necessary to evaluate the time constant in order to estimate the response time of living cells in the electric field (E -field). In the present study, the time constant is evaluated by considering the hypothesis of electrical analog of spherical shaped cells and assuming realistic values for capacitance and resistivity properties of cell/nuclear membrane, cytoplasm, and nucleus. In addition, the resistance of cytoplasm and nucleoplasm was computed based on simple geometrical considerations. Importantly, the analysis on the basis of first principles shows that the average values of time constant would be around 2–3 μ s, assuming the theoretical capacitance values and the analytically computed resistance values. The implication of our analytical solution has been discussed in reference to the cellular adaptation processes such as atrophy/hypertrophy as well as the variation in electrical transport properties of cellular membrane/cytoplasm/nuclear membrane/nucleoplasm. © 2009 American Institute of Physics. [DOI: 10.1063/1.3086627]

I. INTRODUCTION

In the area of biomedical engineering, one of the important aspects is to investigate the influence of external field (electric, magnetic, and electromagnetic) on the *in vitro*, *in vivo*, or *ex vivo* cell fate processes (cell proliferation, cell differentiation, etc.) or tissue formation. In the past, a number of experimental studies have been conducted to probe into such aspect.^{1–4} Such a study has major relevance to tailor the effect of external field on the cell proliferation on new biomaterial surfaces.^{5–10} Since the cell fate processes under the external stimulation involve the interaction of external field with biological cells dispersed in extracellular matrix (ECM), it is important to initially understand such interaction for a single cell. Also, the evaluation of the time scale for such fundamental interaction requires careful theoretical analysis, as precise experimental measurements can be difficult. At a much finer scale, one has to consider how the electric current path will be influenced by the electric transport properties of cell membrane, cytoplasm, nuclear membrane, nucleoplasm, etc.

Typically, a biological cell contains various ions such as K^+ , Na^+ , Cl^- , Ca^{+2} , etc. All such ions are also present in ECM, however, with different concentration. As ECM and cytoplasm have different chemical composition/chemistry, the conductivity of the two medium will also differ and hence, the mobilities of the ions. A dielectric membrane surrounds the cellular organelles as well as all the inorganic ions and organic compounds. As a potential difference is maintained due to the presence of the ions across the dielectric cell membrane, the interaction of the cellular field with the external electric fields is to be expected. If the membrane

potential difference reached in the range of 0.7–1 V in response to externally applied E -field, structural changes in the membrane occur with the transient pore formation across the membrane, a process known as electroporation.^{11,12} Electroporation is one of the mechanisms for transportation of ions and biological molecules between the extracellular matrix and intracellular fluids. Electroporation is also important for cell fusion, drug release, and transport of hydrophilic compounds.¹³ Apart from pore formation in the membrane,¹⁴ dielectrophoresis¹⁵ directed cell shape changes¹⁶ and cell rotation¹⁷ have also been reported as the biophysical changes in the presence of an external electric field. The effect of electric field depends on the pulse duration, field strength, and cell type.^{17,18}

Although the influence of electric field on various biophysical and biochemical processes is known or clinically realized, the fundamental understanding of interaction of electric field with single cell is still missing. In the present work, we attempt to simulate the electrical analog of cells by passive electrical parameters and subsequently evaluate time constant. The concept of time constant can be used to predict the electroporation from the cells, which may be helpful in modifying the endogenous electric field inside the cell. In the process, we have modeled an equivalent circuit for the biological cell. In our study, we have considered a fairly simple cell model with nucleus as the only organelle. We used the electrical equivalent of this cell model to evaluate the cell time constant. Both the cell and the nucleus are taken to be spherical and concentric to each other. Using geometrical approaches, we have analytically determined the resistance of the cytoplasm and nucleoplasm. Subsequently, the influences of cell size and resistance/capacitance of organelle/membrane on the time constant were evaluated analytically.

^{a)}Author to whom correspondence should be addressed. Electronic mail: bikram@iitk.ac.in. Tel.: 00915122597771. FAX: 00915122597505.

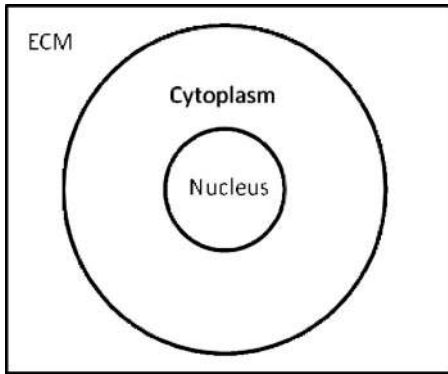


FIG. 1. Schematic representation of the cross section of an ideal spherical biological cell embedded in ECM.

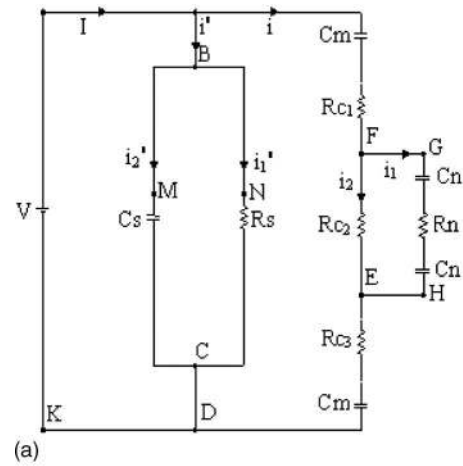
II. MODEL ASSUMPTIONS

In order to develop a simplistic model of electrical analog for a biological cell, a number of assumptions are made.

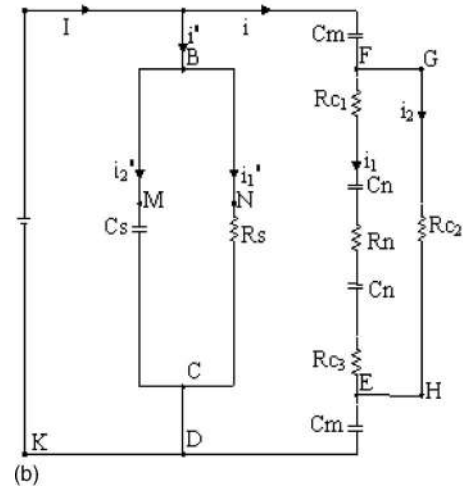
- The near spherical nature of the cell and nucleus is considered. For obtaining an analytical value of resistance, finite deviation of 5° from the spherical symmetry is assumed.
- The resistivity of cytoplasm and nucleoplasm is considered identical.
- The capacitance per unit area of the cell membrane and nuclear membrane is considered equal to each other.
- Although a biological cell contains a number of organelles, only the presence of nucleus is assumed and the presence of other organelles in cytoplasm, e.g., golgi apparatus, mitochondria is neglected.
- The conductivity of the cell membrane and nuclear membrane is neglected.
- The entire analysis holds only in situations prior to the onset of electroporation. Once electroporation initiates at high electric field, the membrane resistance changes dynamically and the present analysis cannot be directly applied.

III. MODEL DESCRIPTION

The cross section of a spherical cell, embedded in ECM, is shown in Fig. 1. Electrical charges are accumulated on the surface of the cell as well as on the nuclear membrane. Consequently, a voltage is developed due to the resulting current generated by externally applied electric field. Because of insulating nature of membrane, the membrane has been treated like a capacitor. Also, cytoplasm and nucleoplasm have been treated like a resistor. To calculate the time constant of the cell, we have considered two electric equivalents of the cell [Figs. 2(a) and 2(b)]. Consequently, two different equivalent circuits were analyzed. While, model 1 was proposed by Deng *et al.*,¹⁹ we have proposed model 2 with a few modifications in model 1. It can be noted that Deng *et al.*¹⁹ did not make any attempt to analytically compute the time constant values. The basic difference between model 1 and model 2 is difference in the ion paths considered. In model 2, we have considered three paths: a path only through the cytoplasm,



(a)



(b)

FIG. 2. (a) Equivalent electrical analog of cell (model 1) after Deng *et al.* [19]. (b) Equivalent electrical analog of cell for model 2.

one from both cytoplasm and nucleoplasm, and the third from the ECM. The difference in ion path essentially implicates the corresponding differences in the current path.

In Figs. 2(a) and 2(b), C_s and R_s are the capacitance and resistance of ECM, respectively, C_m and C_n are the capacitance of cell and nuclear membrane, respectively, and R_{c1} , R_{c2} , and R_{c3} are resistances of different spatial regions of cytoplasm.

A. Time constant calculation

For both models 1 and 2, we have applied the fundamental Kirchhoff's laws at various nodes and the first principle analysis for various circuit components is adopted to solve the current flow. In reference to model 1 [see Fig. 2(a)], applying Kirchhoff's current law at the nodes A, B, and F, we have

$$I = i + i', \quad (1)$$

$$i' = i'_1 + i'_2, \quad (2)$$

$$i = i_1 + i_2. \quad (3)$$

Applying Kirchhoff's voltage law in the loops EFGHE, one can obtain

$$i_2 R_{c2} = i_1 R_n + (2/C_n) \int_0^t i_1 dt. \quad (4)$$

Again, the application of Kirchhoff's voltage law in the loops JAFEDKJ results in the following expression:

$$V = \left(\frac{2}{C_m} \right) \int_0^t idt + i(R_{c1} + R_{c3}) + i_2 R_{c2}. \quad (5)$$

Using these basic circuit equations, we can arrive at the following equation:

$$I = \alpha e^{k_1 t} + \beta e^{k_2 t} + k + \frac{V}{R_s}, \quad (6)$$

where

$$\alpha = A_1 + \frac{A_1 R_n}{R_{c2}} + \frac{2A_1}{R_{c2} C_n k_1},$$

$$\beta = A_2 + \frac{A_2 R_n}{R_{c2}} + \frac{2A_2}{R_{c2} C_n k_2},$$

$$k = -\frac{2A_1}{R_{c2} C_n k_1} - \frac{2A_2}{R_{c2} C_n k_2}.$$

Comparing the exponential term with $i = i_0 e^{-t/\tau}$, we can find that time constants for the circuit shown in Fig. 2(a) are $(-1/k_1)$ and $(-1/k_2)$. Hence,

$$\tau_1, \tau_2 = \frac{-C_n C_m (R_n R_c + R_{c2} R_c - R_{c2}^2)}{-(R_{c2} C_n + R_n C_n + R_c C_m) \pm \sqrt{(R_{c2} C_n + R_n C_n - R_c C_m)^2 + 4R_{c2}^2 C_n C_m}}. \quad (7)$$

Similar calculation for model 2 [Fig. 2(b)] yields the values of time constants as below,

$$\tau_1, \tau_2 = \frac{-C_n C_m R_{c2} R_c}{-(R_{c2} C_n + R_c C_n + R_{c2} C_m) \pm \sqrt{(R_{c2} C_n + R_c C_n - R_{c2} C_m)^2 + 4R_{c2}^2 C_n C_m}}. \quad (8)$$

In both the above cases, the values of τ_1 and τ_2 are always real and positive.

IV. RESULTS AND DISCUSSION

We consider the cytoplasm and the nucleoplasm to be homogeneous fluids. The cell membrane and the nuclear membrane are considered to behave as capacitors while the fluids, i.e., the cytoplasm and nucleoplasm, as resistors.

The resistivity of the cytoplasm and the nucleoplasm is assumed to be the same and equal to 100 Ω cm. The capacitance per unit area of the cell membrane and the nuclear membrane is equal to 1 $\mu\text{F}/\text{cm}^2$.¹⁹ The radius of the cell is taken to be 25 μm . For the purpose of our calculation, we have taken the volume of the nucleus to be one tenth of the volume of the whole cell. Therefore, the nuclear radius (r_n) for the given cell radius (r_c) of 25 μm is computed to be 11.6 μm . In Sec. IV A, we report the variation in various parameters as a function of both r_n and r_0 .

A. Model 1: Calculation of resistance and capacitance values

In order to obtain values of τ_1 and τ_2 [see Eqs. (7) and (8)], it is imperative to know the values of various resistance parameters. In the following, the resistance values are analytically obtained. Figure 3 shows the resistances of the different parts of the cell, which are encountered during the ion transportation in model 1. For a perfect sphere, the resistance is infinite and therefore, to obtain a numerical solution of the time constant, we have considered a finite deviation of 5°

from the exact spherical geometry. This assumption is valid physically as biological cells mostly deviate from the perfect spherical nature. In the Appendix, the estimation of the resistance values from simple geometrical considerations will be illustrated.

The cytoplasm resistance can be computed by considering various spatial resistances (R_{c1} , R_{c2} , and R_{c3}) to be in series,

$$R_c = R_{c1} + R_{c2} + R_{c3}.$$

All the spatial resistances are computed by adopting the geometrical approaches/symmetry and applying the following fundamental relationship:

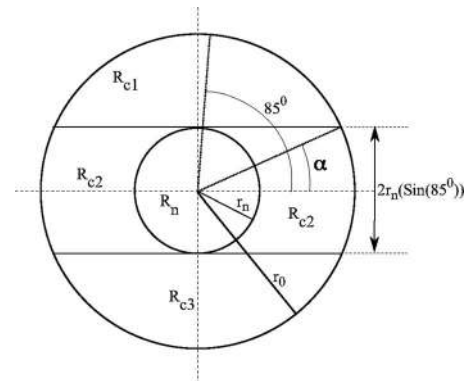


FIG. 3. Geometry illustrating the distribution of the resistances in model 1.

$$R = \frac{\rho l}{A},$$

where l is the length of geometrical segment and A is the cross sectional area of the given segment. The value of ρ is considered to be uniform in the cytoplasm and independent of spatial region. The detailed calculation to obtain values of R_{c1} , R_{c2} , and R_{c3} can be found in the Appendix. From the computed values, the value of cytoplasm and nucleoplasm resistances is obtained as 82.14 and 174.24 K Ω , respectively.

Reiterating the assumption that both cell membrane and nuclear membrane have the same capacitance per unit area, the total membrane capacitance can be calculated as follows:

$$C_m = c(4\pi r_0^2) = 7.85 \times 10^{-11} \text{ F},$$

$$C_n = c(4\pi r_n^2) = 1.69 \times 10^{-11} \text{ F}.$$

Therefore, upon substituting the values of resistances and capacitances in Eq. (7), we obtain the numerical values of the two time constants as follows:

$$\tau_1 = 3.26 \text{ } \mu\text{s} \quad \text{and} \quad \tau_2 = 1.55 \text{ } \mu\text{s}.$$

B. Model 2: Calculation of resistance and capacitance values

Similar to model 1, it is imperative to first calculate the values of various resistance parameters. Figure 4 shows the resistances of the different parts of the cell, which are encountered during the ion transportation in model 2. In the Appendix, the resistance values are analytically obtained. Using simple geometrical approaches and adopting the symmetry aspect, the resistance values are obtained as follows:

$$R_{c1} = R_{c3} = 74.63 \text{ K } \Omega \quad \text{and} \quad R_{c2} = 16.72 \text{ K } \Omega,$$

$$R_n = 174.24 \text{ K } \Omega.$$

Therefore,

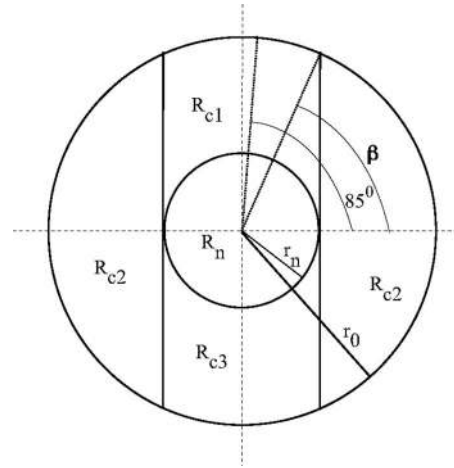


FIG. 4. Geometry illustrating the distribution of the resistances in model 2.

$$R_c = R_{c1} + R_{c3} + R_n = 323.5 \text{ K } \Omega.$$

The capacitance values C_m and C_n of model 2 are the same as the capacitances of model 1,

$$C_m = 7.85 \times 10^{-11} \text{ F} \quad \text{and} \quad C_n = 1.69 \times 10^{-11} \text{ F}.$$

Therefore, upon substituting the values of resistances and capacitances in Eq. (8), we obtain $\tau_1 = 2.8 \text{ } \mu\text{s}$ and $\tau_2 = 0.52 \text{ } \mu\text{s}$. The values of time constant, as obtained above, are deterministic in nature. It can be mentioned here that the realistic interaction of current path with various cellular micro-organelles would evidently modify the time constant values.

C. Model implications

From Eqs. (7) and (8), it is clear that the time constant of cell depends on various cell parameters. We observe that three independent sets of parameters for the cell are important and they include radius of the cell, resistance of the cytoplasm and nucleoplasm, as well as the capacitance of the cell and nuclear membranes. Using MATLAB, the influence of all these parameters on time constant is analytically investi-

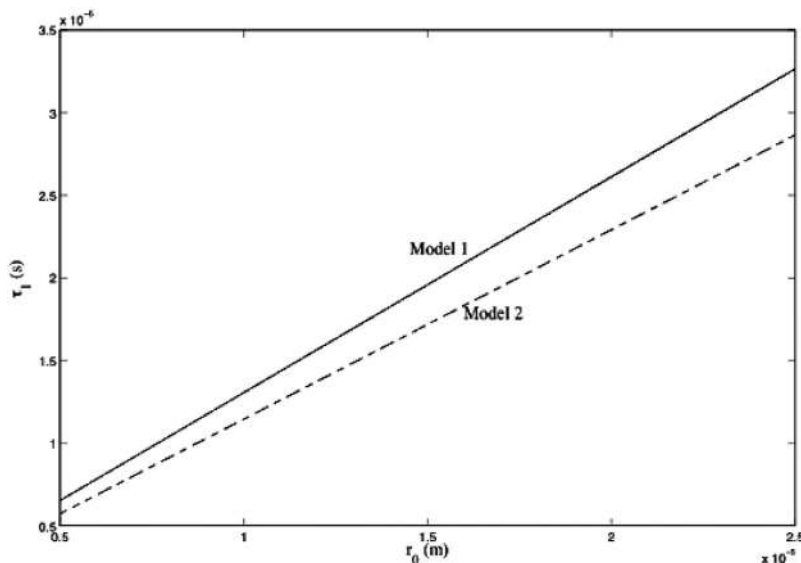


FIG. 5. Plot of time constant (τ_1) versus cell size for both the models.

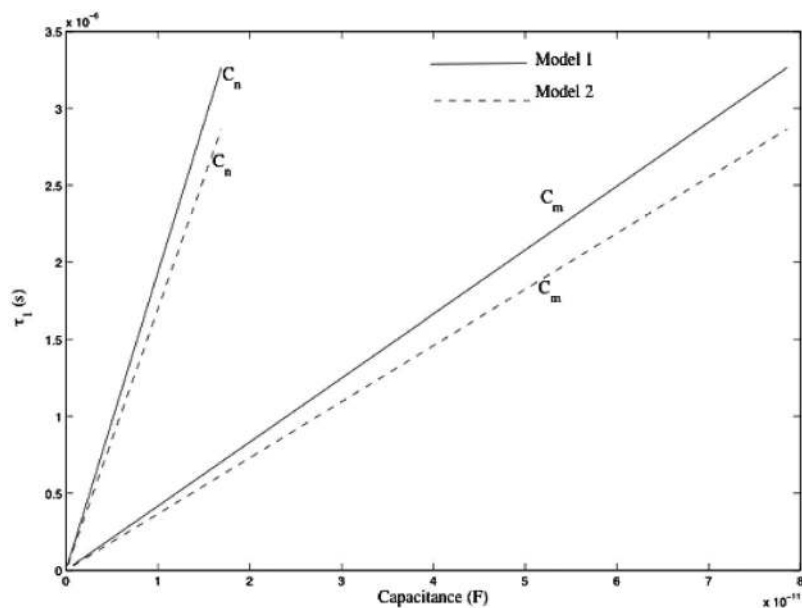


FIG. 6. Plot of time constant (τ_1) versus capacitance of cell membrane (C_m) and time constant (τ_1) versus nuclear membrane (C_n) for Model 1 and Model 2 keeping the radius of cell constant while varying capacitance per unit area.

gated for a given cell type. The variation in time constant (τ_1) with the radius of cell is observed to be linear for both the models, as shown in Fig. 5. For this purpose, we have kept the ratio of r_n/r_o to be equal to 0.46. This assumption is based on the fact that volume of the nucleus is typically reported to be one tenth of the volume of the entire cell.²⁰ From Fig. 5, it is clear that model 1 predicts more rapid change in the time constant values with the cell radius. From the fundamental theory of cell-material interaction, it is known that any biological cell initially interacts with proteins adsorbed on a biomaterial.²¹ During the process of interaction, a cell eventually spreads with time and as a result, the cell undergoes the shape and size change. In addition, during the cellular adaptation process, cells can undergo atrophy (decrease in size) or hypertrophy (increase in size). In view of the present observations, it can therefore be said that the interaction time of the electrical pulse will increase during the adhesion of a given cell type.

In Fig. 6, the variation in τ_1 with the capacitance of the nuclear and cell membrane for both the models has been plotted. For obtaining these results, the radius of the cell was kept constant, while the capacitance per unit area of the membranes was varied. Although a linear relationship between time constant and C_n or C_m was observed, the variation with C_n was found to be steeper. Therefore, a small change in C_n value can cause more rapid change in time constant, compared to that in case of C_m . Linear variation of the time constant with C_m and C_n can be explained by the fact that first order linear circuit assumption has been considered for both the nuclear and cellular membranes. As per our assumption, the capacitance per unit area of both nucleus and cell membrane is equal and if one follows Eqs. (7) and (8) closely, the linear dependence of time constant with capacitance will clearly emerge. It needs to be pointed out here that such linear relationship will hold true as far as the assumption of neglecting the conductivity of the membranes is valid. With the onset of the electroporation, the linear relationship will be disturbed because of the transportation of the ions across the cell membrane.

Figure 7 illustrates the variation in time constant (τ_1) with various resistances of the equivalent circuit for both the models. τ_1 is observed to vary inversely with all the resistance values in both the cases. From the plotted results, it appears that the variation in nuclear resistance will cause an asymptotic change in time constant values. In case of model 2, although similar variation in τ_1 with resistance is noted, the decrease in τ_1 with nuclear resistance is much slower than that with cytoplasm resistance. As far as the influence of cytoplasm resistance is concerned, model 1 predicts a more rapid change in time constant values with a small change in resistance values. It is interesting to note that the plots of τ_2 versus cell size/resistance/capacitance of the cell and nuclear membranes reveal a similar kind of variation for models 1 and 2 (not shown).

Figure 8 shows the variation in time constant with the radius of the cell with various r_n/r_o values ranging from 0.2 to 0.8. It has been observed that as the ratio of r_n/r_o increases, the time constant (τ_1) also increases. From Fig. 8, we can conclude that if the value of r_o is kept constant, the time constant (τ_1) also increases with increase in r_n .

The present work has major implications on the following aspects. Any experimental study to probe into the cell-material interaction can use short electrical pulses of microsecond pulse width. Also, the less chances of any cellular damage with electrical pulse width of less than a microsecond can be predicted. In order to realize the external electric field on wound damage repair involving cellular adaptation process, one has to use electrical pulses of microsecond or larger. However, in order to obtain a more rigorous solution for electrical analog of biological cells with multiple cellular organelles, further analytical/computational study is required. Also required is the estimation of the time constant values for the case of multiple cells dispersed in ECM, as this will be the situation close to the realistic case of a biological tissue. Nevertheless, the present study can be consid-

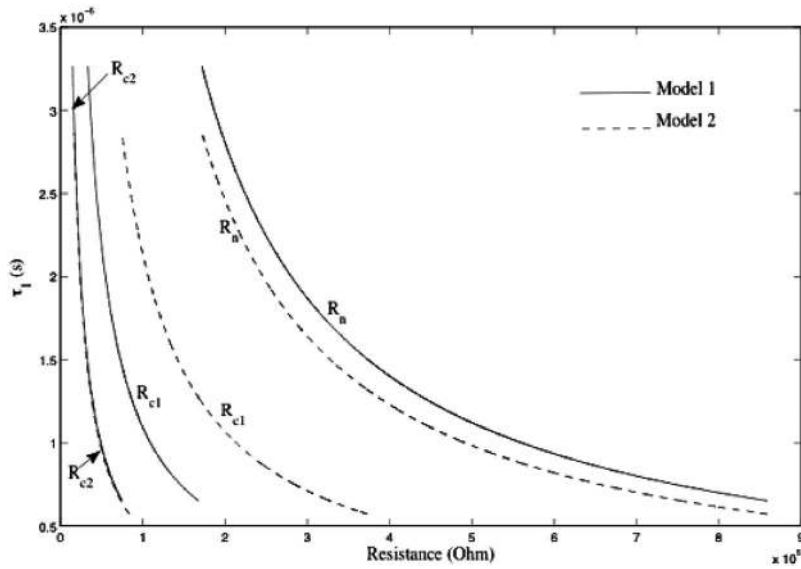


FIG. 7. Plot of time constant of the cell (τ_1) versus resistance of cytoplasm (R_{c1} , R_{c2}) and nucleoplasm (R_n) for Model 1 and Model 2.

ered as a preliminary step for further experimental/analytical/computational investigation to probe into the influence of external electric field on cellular response.

Finally, it is instructive to comment on the use of two different models to predict the time constant. In the present work, two different models (models 1 and 2) are proposed on the basis of consideration of two different ion paths or current flow through the entire cell and consequently, two different linear circuits were analyzed. Based on the first principles calculations, it is clear that the time constant values vary within the same order of magnitude (microseconds) for both the models. On closer observations of the data presented in Figs. 5–7, we notice that model 1 overestimates, although to a small extent, the time constant values compared to model 2 for a given cell size or capacitance or

resistance value. However, the model predictions are almost similar under the given set of assumptions.

Typically, the current path/ion flow path follows the least resistance path. In addition, the cell size/shape changes during cellular adaptation processes will also influence the current path. As mentioned earlier, the biological cells, in real life scenario, constantly undergo atrophy or hypertrophy in response to external stimulations/field. From the physical shape aspect, model 2 explains the time constant more precisely in both cases when the cell tends to be more ellipsoidal in nature and nucleus size is much smaller in comparison to cell size (i.e., r_n/r_0 is low).

V. CONCLUSIONS

In the present work, an analytical solution for the time constant for the electrical analog of the biological cell, originally proposed by Deng *et al.*,¹⁹ has been obtained upon application of the first principles theory. In addition, a similar

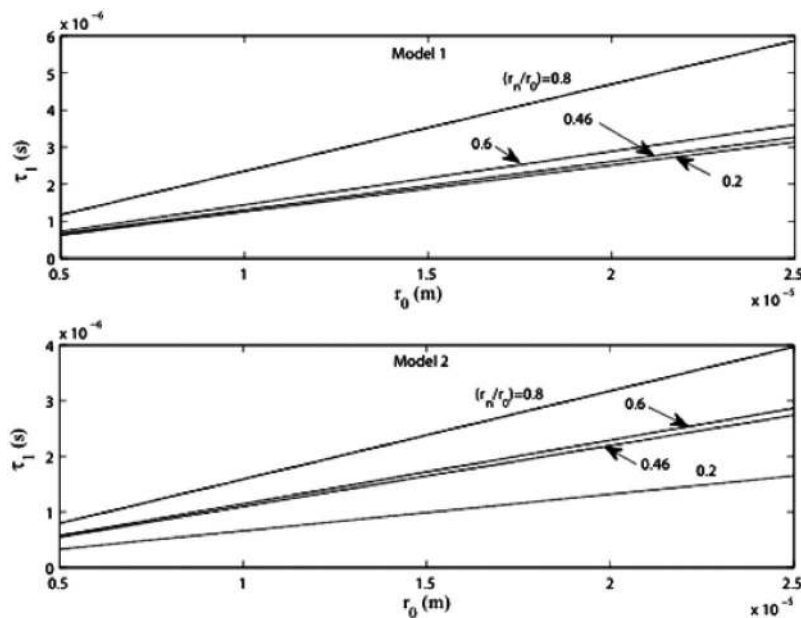


FIG. 8. Plot of time constant with radius of cell with various values of r_n/r_0 values for both Model 1 and Model 2.

solution for a modified electrical analog with slightly different ionic transport path has been achieved. Also, simple geometrical approaches are adopted in the present work to analytically compute the resistance properties of cytoplasm and nucleoplasm for both models. Besides this aspect, the following points emerge as major conclusions:

- The value of the time constant of the cell for both the models has been estimated to vary around 2–3 μs .
- The analytical solutions using MATLAB reveals that the time constant values can linearly increase with the cell size and this will have a major implication on the interaction of the electric field during the cellular adaptation process of atrophy/hypertrophy.
- The variation in capacitance of nuclear membrane has been found to have a much stronger influence on the increase in time constant than the cell membrane.
- The cytoplasm resistance, in contrast to nucleoplasm resistance, is analytically observed to cause a steep decrease in time constant.

APPENDIX: CALCULATION OF THE RESISTANCE VALUES

1. Model 1

a. Calculation of R_{c1}

Referring to Fig. 3, we can write the expression for R_{c1} as following:

$$R_{c1} = \frac{\rho}{\pi r_0} \ln \left(\frac{\sec(85^\circ) + \tan(85^\circ)}{\sec(\alpha) + \tan(\alpha)} \right),$$

where

$$\alpha = \sin^{-1} \left(\frac{r_n \sin(85^\circ)}{r_0} \right) = 27.53^\circ.$$

Finally, we obtain, $R_{c1} = 33.57 \text{ K } \Omega$. Considering the geometrical symmetry, it is clear that $R_{c3} = R_{c1} = 33.57 \text{ K } \Omega$.

b. Calculation of R_{c2}

Referring to Fig. 3, we obtain

$$R_{c2} = \frac{2\rho}{\pi(r_0^2 - r_n^2)} [r_n \sin(85^\circ)],$$

$$R_{c2} = 15 \text{ K } \Omega.$$

Therefore, the total cytoplasm resistance is

$$R_c = R_{c1} + R_{c3} + R_{c2} = 82.14 \text{ K } \Omega.$$

c. Calculation of R_n

Referring to Fig. 3, one can get

$$R_n = \frac{\rho}{\pi r_n} \ln \left[\frac{\sec(85^\circ) + \tan(85^\circ)}{\sec(85^\circ) - \tan(85^\circ)} \right].$$

Therefore, $R_n = 174.24 \text{ K } \Omega$.

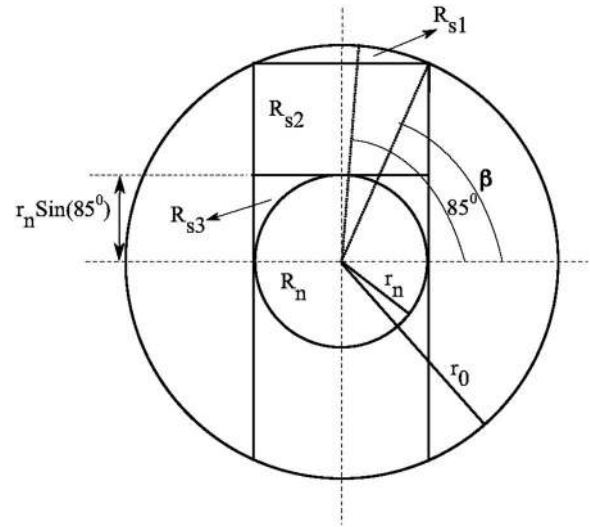


FIG. 9. Geometry illustrating the calculation of cytoplasm resistance (R_{c1}) in Model 2.

2. Model 2

a. Calculation of R_{c1}

Referring to Fig. 9, R_{c1} can be calculated in three steps. This is because R_{s1} , R_{s2} , and R_{s3} are in series with each other,

$$R_{c1} = R_{s1} + R_{s2} + R_{s3}.$$

b. Calculation of R_{s1}

Referring to Figs. 4 and 9, one can get

$$R_{s1} = \frac{\rho}{\pi r_0} \ln \left(\frac{\sec(85^\circ) + \tan(85^\circ)}{\sec(\beta) + \tan(\beta)} \right),$$

where

$$\beta = \cos^{-1} \left(\frac{r_n}{r_0} \right).$$

Therefore, $R_{s1} = 22.04 \text{ K } \Omega$.

c. Calculation of R_{s2}

Again, referring to Figs. 4 and 9, one can write

$$R_{s2} = \frac{\rho}{\pi r_n} [r_0 \sin(\beta) - r_n \sin(85^\circ)].$$

Therefore, $R_{s2} = 25.05 \text{ K } \Omega$.

d. Calculation of R_{s3}

Referring to Figs. 4 and 9, we get

$$R_{s3} = \frac{\rho}{\pi r_n \sin(85^\circ)}.$$

Therefore, $R_{s3} = 27.54 \text{ K } \Omega$. Finally, $R_{c1} = R_{s1} + R_{s2} + R_{s3} = 74.63 \text{ K } \Omega$. From symmetry of the model, $R_{c1} = R_{c3} = 74.63 \text{ K } \Omega$.

e. Calculation of R_{c2}

Referring to Fig. 4, one can write

$$R_{c2} = \frac{2\rho}{\pi r_t} \left(\ln \left| \frac{r_t + r_0 \cos(\beta)}{r_t - r_0 \cos(\beta)} \right| \right),$$

$$R_{c2} = 16.72 \text{ K } \Omega.$$

Referring to Fig. 4, we observe that R_n calculation is the same as in model 1, and therefore we can write

$$R_n = \frac{\rho}{\pi r_n} \ln \left(\frac{\sec(85^\circ) + \tan(85^\circ)}{\sec(85^\circ) - \tan(85^\circ)} \right),$$

$$R_n = 174.24 \text{ K } \Omega.$$

¹L. Dini and L. Abbro, *Micron* **36**, 195 (2005).

²W. O. Short, L. Gookwill, C. W. Taylor, C. Job, M. E. Arthur, and A. E. Cress, *Invest. Radiol.* **27**, 836 (1992).

³V. Ottani, M. Raspanti, D. Martini, G. Tretola, A. Ruggeri, Jr., M. Franchi, G. G. Piccari, and A. Ruggeri, *Micron* **33**, 121 (2002).

⁴D. J. Panagopoulos, N. Messini, A. Karabarbounis, A. L. Philippetis, and L. H. Margaritis, *Biochem. Biophys. Res. Commun.* **272**, 634 (2000).

⁵S. Nath and B. Basu, *J. Korean Ceram. Soc.* **45**, 1 (2008).

⁶S. Roy and B. Basu, *J. Mater. Sci.: Mater. Med.* **21**, 51 (2008).

⁷S. Roy and B. Basu, *J. Mater. Sci.: Mater. Med.* **19**, 3123 (2008).

⁸S. Nath, S. Bodhak, and B. Basu, *J. Biomed. Mater. Res.* **83**, 191 (2007).

⁹S. Nath, R. Tripathi, and B. Basu, *Mater. Sci. Eng., C* **29**, 97 (2009).

¹⁰S. Nath, S. Bajaj, and B. Basu, *Int. J. Appl. Ceram. Technol.* **5**, 49 (2008).

¹¹J. C. Weaver, in *The Biomedical Engineering Handbook*, edited by J. D. Bronzino (CRC, Boca Raton, FL, 1995), pp. 1431–1440.

¹²S. B. Dev, D. P. Rabussay, G. Widera, and G. A. Hofmann, *IEEE Trans. Plasma Sci.* **28**, 1 (2000).

¹³U. Pliquet, R. P. Joshi, V. Sridhara, and K. H. Schoenbach, *Biochemistry* **70**, 275 (2007).

¹⁴E. Neumann and K. Rosenheck, *J. Membr. Biol.* **10**, 279 (1972).

¹⁵F. A. Sauer, in *Coherent Excitations in Biological Systems*, edited by H. Frohlich and F. Kremer (Springer-Verlag, Berlin, 1983).

¹⁶E. K. Onuma and S. W. Hui, *J. Cell Biol.* **106**, 2067 (1988).

¹⁷W. M. Arnold and U. Zimmermann, *Biological Membranes* (Academic, New York, 1984), Vol. 5, p. 389.

¹⁸A. L. Garner, G. Chen, N. Chen, V. Sridhara, J. F. Kolb, R. J. Swanson, S. J. Beebe, R. P. Joshi, and K. H. Schoenbach, *Biochem. Biophys. Res. Commun.* **362**, 139 (2007).

¹⁹J. Deng, K. H. Schoenbach, E. S. Buescher, P. S. Hair, P. M. Fox, and S. J. Beebe, *Biophys. J.* **84**, 2709 (2003).

²⁰B. Alberts, A. Johnson, J. Lewis, M. Raff, K. Roberts, and P. Walter, *Molecular Biology of the Cell*, 5th ed. (Taylor & Francis, London, 2007).

²¹B. Ratner, A. S. Hoffman, F. J. Schoen, and J. E. Lemons, *Biomaterials Science: An Introduction to Materials in Medicine* (Academic, New York, 1996).

Journal of Applied Physics is copyrighted by the American Institute of Physics (AIP).
Redistribution of journal material is subject to the AIP online journal license and/or AIP
copyright. For more information, see <http://ojps.aip.org/japo/japcr/jsp>